RESPONSE OF THE PRIMARY PIPING LOOP TO AN HCDA

Y.W. CHANG, M.T.A. MONEIM, C.Y. WANG, and J. GVILDYS

Reactor Analysis and Safety Division,
Argonne National Laboratory, Argonne, Illinois 60439, U.S.A.

SUMMARY

The paper describes a method for analyzing the response of the primary piping loop that consists of straight pipes, elbows, and other components connected in series and subject to hypothetical core disruptive accident (HCDA) loads at both ends of the loop. The complete hydrodynamic equations in two-dimensions, that include both the nonlinear convective and viscous dissipation terms are used for the fluid dynamics together with the implicit ICE technique. The external walls of the pipes and components are treated as thin shells in which the analysis accounts for the membrane and bending strength of the wall, elastic-plastic material behavior, as well as large deformation under the effect of transient loading conditions.

The fluid dynamics and the shell deformation are calculated separately in two calculations, but they interact every cycle by supplying each others required boundary conditions at the common boundary. For the shell motion, it uses a pressure boundary condition in which the pressure loads are obtained from the fluid dynamics calculations. In the fluid calculations, the fluid at the wall boundary is allowed to slip along the wall, but forced to move together in the direction normal to the wall.

The elbow analysis utilizes a two-dimensional model that ignores the secondary motion in the elbow and considers the flow in the r-direction, radially outward from the center of curvature, and the tangential θ-direction. The other components are modeled as a cylinder of larger diameter, in which the radius of the cylinder can be varied to conform with the outside shape of the component. The flow area inside the cylinder can be reduced or increased independently from the outside shape, to accommodate the actual flow area. However, they must remain axial symmetric. The elbow walls are considered to be rigid, but the external walls of the other components can be treated as rigid or elastic-plastic.

Finally, the method is applied to a piping loop which consists of six elastic-plastic pipes and five rigid elbows connected in series and subjected to pressure pulses at both ends of the loop. The results show (1) how the pressure pulses are attenuated as the pipe wall deforms, (2) how the attenuated pressure pulses meet at the vicinity of the middle of the loop to produce a second pulse which causes the pipe wall to deform plastically in that vicinity, (3) how more plastic deformations of the pipe walls are formed as the second pulse moves in both directions toward both ends of the loop, and (4) how the pressure near the outer and inner walls of the elbow is affected by the centrifugal forces which is ignored in the one-dimensional analysis.

1. Introduction

The high-pressure pulses generated in a hypothetical core-disruptive accident (HCDA) can propagate through piping loops of the primary coolant system and may cause damage to loop components. The safety assessment of the reactor design requires an analysis of the capability of the primary piping loop to sustain the consequences of such an accident, even though it is a hypothetical one.

The conventional methods used for the safety analysis on the dynamic response of the primary piping loop under HCDA pressure pulses are mostly one-dimensional. They treat the primary loop as a series of finite-length pipes connected at joints, where the elbows, valves, and other components are replaced by single finite-length pipes with equivalent flow areas. The effect of plastic deformations of the pipe wall is either totally ignored, or treated as an increase of the fluid compressibility. The pressure loadings predicted by these methods are not adequate for safety evaluation.

This paper describes a method for analyzing the response of the primary piping loop under HCDA loadings. The piping loop consists of straight pipes, elbows, and other components. The complete hydrodynamic equations in two dimensions that include both the nonlinear convective and viscous dissipation terms are used for the fluid dynamics. The external walls of the pipes and components are treated as thin shells in which the analysis accounts for the membrane and bending strength of the wall, elastic-plastic material behavior, and large deformations under transient loading conditions.

In the straight pipes, the flow is assumed to be axisymmetric; in the elbow regions, the two dimensions considered are the r and θ directions. The flow in the other components is also assumed to be axisymmetric; the components are modeled as a circular cylinder, in which the radius of the cylinder can be varied to conform with the outside shape of the component and the flow area inside can be changed independently from the outside shape. However, they must remain axially symmetric.

In the analysis, the differential equations of mass, momentum, and energy, and equation of state are approximated by finite-difference equations and solved numerically on the computer. For the fluids, they are expressed in the Eulerian coordinates; for the shells, in the Lagrangian coordinates.

2. Mathematical Model

2.1 Axisymmetric Model

The flow in the straight pipes, valves, and other components (except elbows) is considered to be axisymmetric. The fluid is considered to be viscous and compressible, but non-heat-conducting. The conservation equations of mass, momentum, and energy are:

$$\frac{\partial \rho}{\partial t} + \frac{1}{r}\frac{\partial \rho u r}{\partial r} + \frac{\partial \rho v}{\partial z} = 0 , \tag{1}$$

$$\frac{\partial \rho u}{\partial t} + \frac{1}{r}\frac{\partial \rho u^2 r}{\partial r} + \frac{\partial \rho u v}{\partial z} = -\frac{\partial}{\partial r}(p + q) + \mu\frac{\partial}{\partial z}\left(\frac{\partial u}{\partial z} - \frac{\partial v}{\partial r}\right) , \tag{2}$$

$$\frac{\partial \rho v}{\partial t} + \frac{1}{r}\frac{\partial \rho u v r}{\partial r} + \frac{\partial \rho v^2}{\partial z} = -\frac{\partial}{\partial z}(p + q) - \frac{u}{r}\frac{\partial}{\partial r}\left[r\left(\frac{\partial u}{\partial r} - \frac{\partial v}{\partial r}\right)\right] , \tag{3}$$

$$\frac{\partial \rho E}{\partial t} + \frac{1}{r}\frac{\partial \rho u E r}{\partial r} + \frac{\partial \rho v E}{\partial z} = + \frac{1}{r}\frac{\partial}{\partial r}\left\{ r\left[- pu - \left(\frac{\lambda}{\lambda + 2\mu}\right) qu + \frac{\mu}{2}\frac{\partial}{\partial r}(2u^2 + v^2) + \mu v \frac{\partial u}{\partial z}\right]\right\} + \frac{\partial}{\partial z}\left\{ - pv - \left(\frac{\lambda}{\lambda + 2\mu}\right) qv + \frac{\mu}{2}\frac{\partial}{\partial z}(u^2 + 2v^2) + \mu u \frac{\partial v}{\partial r}\right\} . \qquad (4)$$

in which r and z denote the Eulerian coordinations, ρ is the density, u and v denote the component of the radial and axial velocity, respectively, t is the time, p is the pressure, $E = I + (u^2 + v^2)/2$, with I the specific internal energy, and $q = -(\lambda + 2\mu)\left(\frac{1}{r}\frac{\partial ur}{\partial r} + \frac{\partial v}{\partial z}\right)$, with λ and μ the viscosity coefficients. These viscosity coefficients can be used as artificial viscosities to eliminate the shock discontinuities and numerical instability.

The location of these variables in a Eulerian computational cell is shown in fig. 1. The equation of state is assumed to have the form

$$\rho = f(p,I) \quad . \qquad (5)$$

The external walls of the pipes and components are treated as thin shells. The equations of motion are:

$$\begin{aligned} &\frac{\partial}{\partial s}\left[N_\phi r\cos\phi\right] - \frac{\partial}{\partial s}\left[Q_\phi r\sin\phi\right] - N_\theta + pr\sin\phi - mr\ddot{r} = 0 \quad , \\ &\frac{\partial}{\partial s}\left[N_\phi r\sin\phi\right] + \frac{\partial}{\partial s}\left[Q_\phi r\cos\phi\right] - pr\cos\phi - mr\ddot{z} = 0 \quad , \qquad (6) \\ &\frac{\partial}{\partial s}\left[M_\phi r\right] - M_\theta\cos\phi - Q_\phi r = 0 \quad , \end{aligned}$$

where s is the length of the shell, m the mass of the shell per unit area, ϕ the angle of inclination of the element with respect to the r-direction, p the pressure, N_ϕ and N_θ two tangential forces, Q_ϕ the transverse force, and M_ϕ and M_θ the two bending moments. The shell material is considered to be elastic-plastic, strain-hardening, and strain-rate sensitive. The von Mises yield condition and the incremental strain theory of plasticity are used.

2.2 Elbow Model

The analysis of the transient fluid dynamics in the elbow requires the development of a three-dimensional model. However, a two-dimensional model can be developed to approximate the transient flow in the elbow if the secondary flow in the elbow is small and can be ignored. The two dimensions considered are the radial r-direction, radially outward from the center of curvature of the elbow, and the tangential θ-direction, as shown in fig. 2, where the Eulerian mesh of the elbow is also shown.

The conservation equations of mass, momentum, and energy are:

$$\frac{\partial \rho}{\partial t} + \frac{1}{r\eta}\frac{\partial (r\ell\rho u)}{\partial r} + \frac{1}{r}\frac{\partial (\rho v)}{\partial \theta} = 0 \quad , \qquad (7)$$

$$\frac{\partial(\rho u)}{\partial t} + \frac{u}{\eta}\frac{\partial(\ell\rho u)}{\partial r} + \frac{1}{r}\frac{\partial(\rho uv)}{\partial\theta} + \rho\left(\frac{1}{2}\frac{\partial u^2}{\partial r} - \frac{v^2}{r} + \frac{u^2\ell}{r\eta}\right) =$$

$$\frac{p}{r} - \frac{\ell}{\eta}\frac{\partial}{\partial r}\left(p + \frac{\lambda q}{\lambda+2\mu} - 2\mu\frac{\partial u}{\partial r}\right) + \frac{\lambda}{\lambda+2\mu}\frac{q}{r} + \frac{1}{r}\frac{\partial}{\partial\theta}\left(H - \frac{2\mu v}{r}\right) - 2\mu\frac{u}{r^2} \quad , \tag{8}$$

$$\frac{\partial(\rho v)}{\partial t} + \frac{v}{\eta}\frac{\partial(\ell\rho u)}{\partial r} + \frac{\rho u}{r}\frac{\partial(rv)}{\partial r} + \frac{1}{r}\frac{\partial(\rho v^2)}{\partial\theta} + \frac{\rho uv\ell}{r\eta} =$$

$$-\frac{1}{r}\frac{\partial}{\partial\theta}(p+q) + \frac{1}{r\eta}\frac{\partial(r\ell H)}{\partial r} + \frac{H}{r} + \frac{2\mu}{r^2}\frac{\partial}{\partial\theta}\left(u - \frac{1}{\eta}\frac{\partial(ru\ell)}{\partial r}\right)$$

$$-2\mu\frac{\xi(r)}{\eta}\left|\frac{R-r}{r_o}\frac{\partial v}{\partial r}\right|\frac{|v|}{v} \quad , \tag{9}$$

$$\frac{\partial(\rho E)}{\partial t} + \frac{1}{r}\frac{\partial(\rho vE)}{\partial\theta} + \rho u\frac{\partial E}{\partial r} + \frac{E}{r\eta}\frac{\partial(\rho ru\ell)}{\partial r} =$$

$$\frac{1}{r\eta}\frac{\partial}{\partial r}\left[r\ell\left\{-pu - \frac{\lambda}{\lambda+2\mu}qu + 2\mu u\frac{\partial u}{\partial r} + vH\right\}\right] \tag{10}$$

$$+\frac{1}{r}\frac{\partial}{\partial\theta}\left[-pv - \frac{\lambda}{\lambda+2\mu}qv + 2\mu v\left(\frac{1}{r}\frac{\partial v}{\partial\theta} + \frac{u}{r}\right) + uH\right]$$

$$-2\mu\frac{\xi(r)}{\eta}\left|\frac{R-r}{r_o}\frac{\partial v}{\partial r}v\right| \quad ,$$

where ℓ is the length of the cord of the circular cross-section of the elbow, r_o the radius of the cross section of the elbow, R the radius of the curvature of the elbow, u and v the radial and tangential velocity components, and

$$q = -(\lambda+2\mu)\left(\frac{1}{r\eta}\frac{\partial(ru\ell)}{\partial r} + \frac{1}{r}\frac{\partial v}{\partial\theta}\right) \quad ,$$

$$H = \mu\left[r\frac{\partial}{\partial r}\left(\frac{v}{r}\right) + \frac{1}{r}\frac{\partial u}{\partial\theta}\right] \quad ,$$

$$\eta = \frac{A_\theta}{\delta r} \quad \text{(refer to fig. 2)} \quad ,$$

$$\xi(r) = \frac{A_w}{r\delta r\delta\theta} = 1 + \frac{1}{2}\left(\frac{r-R}{r_o}\right)^2 + \frac{1.3}{2.4}\left(\frac{r-R}{r_o}\right)^4 + \frac{1.3.5}{2.4.6}\left(\frac{r-R}{r_o}\right)^6 + \cdots\cdots,$$

with

A_θ = Eulerian zone area normal to the θ-direction

A_w = elbow wall area

δ_r = interval size in the r-direction

δ_θ = interval size in the θ-direction

The detail derivation of these equations is given in [1]. The elbow wall is assumed to be rigid.

3. Numerical Technique

The numerical technique used for the fluid calculation is the implicit ICE technique developed by Harlow and Amsden [2]. Briefly, the nonlinear differential equations of mass, momentum, and energy, and equations of state are approximated by the finite-difference equations with respect to the Eulerian cell. Substitutions of the unknown advanced-time densities and velocities into the difference form of the mass equation results in a set of Poisson's equations in the advanced-time pressures. These pressures are solved iteratively

on the computer. After the advanced-time pressures are obtained, the new densities, velocities, and energies are evaluated, using the equations of state, and momentum and energy equations, respectively.

The shell calculation is done separately using the numerical technique as described in [3], but it interacts with the fluid calculation in each time step by supplying the fluid dynamics with a moving boundary condition. In return, the fluid dynamics calculation supplies the shell with a pressure loading condition. The pressure in the fictitious zones outside the shell wall is determined in such a way that the fluid is allowed to slide along the wall, but is forced to move together with the wall in the direction normal to the wall. The detail finite-difference equations and computational procedure are given in [4].

4. Coupling of the Axisymmetric Model with the Elbow Model

The basic assumption used in the two-dimensional piping loop analysis is that the flow inside the pipes and other axisymmetric models remains axially symmetric. Because of the shape of the Eulerian zones in the axisymmetric models is different from that in the elbows, the coupling of the two models presents a difficulty in the junctions between these models. As can be seen, in applying the Poisson's equation at the pipe zones next to the junction, one requires a column of fictitious zones outside the pipe. The field variables in these zones are related to the connecting elbow. The same is true for the elbow fictitious zones. However, as mentioned above, the pipe zones are in rings and the elbow zones are in strips. The field variables in the pipe fictitious zones cannot be taken directly from the appropriate elbow zones or vice versa. The technique used here determines the pressure in the fictitious zones in such a way that: (1) the continuity of the mass flow rate across the interconnected ring and strip is satisfied; (2) the total force exerted by the pressures in the fictitious zones of the pipe is equal to the total force exerted by the pressures in the connecting elbow zones; (3) the total force exerted by the pressures in the fictitious zones of the elbow on the junction is equal to the total force exerted by the pressures in the connecting pipe zones. Again, detailed description regarding the coupling process is given in [1].

5. Sample Problems

To illustrate the implicit ICE technique, four sample problems are given. The first problem deals with propagation of HCDA pressure pulse in a plastically deforming pipe to show the effect of wall deformations on wave propagations. Since the same problem was also performed experimentally by Stanford Research Institute (SRI) [5], the experimental results are used here to validate the numerical technique. The second problem deals with the fluid transient in a simple valve system where the mathematical model, as well as the results are discussed. The third problem deals with the elbow. It shows the elbow mathematical model and the effect of the centrifugal force on pressure distribution inside the elbow. The fourth problem deals with the response of a piping loop that consists of six elastic-plastic pipes with five rigid elbows connected in series and subjected to pressure pulses at both ends of the loop.

5.1 Propagation of HCDA Pressure Pulses in a Plastically Deforming Pipe

In the SRI experiment, the pressure pulse was generated by a pulse gun attached to the pipe, as shown in fig. 3. The pipe was 3 in. O.D., 40 mils thick, and 10 ft long, and was filled with water. Figure 4a is the recorded pressure-time history at position 1 (shown in

fig. 3) in the pulse gun, which was used as the source pressure in the numerical calculation.

Figure 4b-d gives the computed pressure-time histories at pipe locations 1A, 2 and 3, along with the mean values of the experimental pulses recorded by SRI. As can be seen from these figures that the pressure pulse has been significantly attentuated by the plastic deformation of the pipe wall. Since the plastic waves travel much more slowly than the elastic waves, the pressure pulse which causes the pipe to yield is noticeably dispersed as it travels to the downstream. It is also noted that the plastic deformations of the pipe are limited to a short length of the pipe near the source pressure. For instance, at $t = 4$ msec, the computed radial deformation of the pipe wall at locations 1C-3C are, respectively, 0.087, 0.074, and 0.0083 cm. The SRI posttest measurement of the corresponding deformations were 0.094, 0.068, and 0.0025 cm. The deviation of the pipe deformation between the two results at location 3C is due to the material properties of the pipe wall, which was approximated by a bilinear curve. Slight deviation of the assumed yield stress value in the numerical analysis can change the wall deformation substantially, if the material is just changed from elastic to plastic. Nevertheless, the solution obtained by the implicit ICE technique agrees well with the experimental results.

5.2 Fluid Transient in a Simple Valve

Figure 5a is the mathematical model in which the valve is modeled as a circular cylinder having a larger cross section than the two connecting pipes. In the analysis, all wall boundaries are assumed to be rigid. It should be mentioned that the use of the rigid wall is not a limitation of the method. This is because the rigid wall solution of that problem can be obtained from a one-dimensional characteristics method which can be used as a comparison with the implicit ICE method. The applied source pressure is given in fig. 5b.

Figure 6 shows the time histories of pressure pulses at locations A and B (shown in fig. 5a), where the results of the one-dimensional characteristics method using the NAHAMMER code [6] are also given. As can be seen the two sets of results are in good agreement.

Although the one-dimensional characteristics method can give satisfactory results, the velocity and pressure losses at the pipe valve junctions must be provided as input information. In the implicit ICE method, they are determined by the fluid dynamics. Also, solution of the implicit ICE method shows that the fluid velocity is not uniform in the valve region. This nonuniform velocity distribution is not calculable by the one-dimensional method.

5.3 Fluid Transient in a Rigid Elbow

The pipe-elbow loop consists of two pipes and one elbow as shown in fig. 7a. For the purpose of illustration, the pipe walls are assumed to be rigid. At one end of the pipe, it is subjected to a pressure pulse as shown in fig. 5b, while the other end is kept open to zero pressure.

Figure 7b shows the pressure histories at locations A and B inside the elbow. It can be seen that the pressure at the outer wall is always higher than the pressure at the inner wall, because of the effect of the centrifugal force. This nonuniform pressure distribution inside the elbow is ignored in the one-dimensional analysis.

5.4 Response of a Piping Loop

The piping loop consists of six elastic-plastic pipes and five rigid elbows connected in series, as shown in fig. 8. Table I gives the dimensions of the components of the loop.

The inlet to the loop is subject to a 50-bar step pressure pulse; the outlet is subject to a 25-bar step pressure pulse; both are of 7 msec duration. The pipe walls are assumed made of elastic-plastic Nickel-200 whose stress-strain curve is approximated by a bilinear curve with a yield stress of 1207 bar. Meanwhile, the elbow walls are considered as rigid.

Figure 9 gives the computed pressure traces at various locations in the loop. In general, the pressure pulses at locations away from the pressure source are reduced by the wall deformation if the pressure source is greater than the yield stress of the pipe, as has been demonstrated in sample problem no. 1. However, this is no longer true in the case of a loop subjected to two pulses at both ends. As can be seen from this sample problem, a second pulse is formed when the two pulses meet at the middle of the loop near location 5. Further pipe wall deformation and interaction with the applied pulses as the reflected wave moves toward the ends causes the pulse in pipe 3 to increase to 54 bars.

This can be further illustrated by the deformation of pipe 4 at various times, given in fig. 10. It shows that at t = 2 msec, the two pulses meet near node 7, at location 5, causing immediate deformation in that vicinity, which is represented by the bulge shown. Soon after, the bulge spreads in both directions, indicating the propagation of the pressure wave in both directions. Later, at t = 5 msec, the configuration indicates that a new pressure wave is moving toward the middle of the pipe. This new pressure wave is the result of the interaction between the reflected pressure wave and the applied pulse.

The results also show that plastic deformation occurs everywhere in the loop except at node 13, where the deformation is elastic. As expected, the pressure near the outer wall of the elbow was found to become higher than the pressure near the inner wall of the elbow, because of the effects of the centrifugal forces.

6. Conclusions and Discussions

It has been demonstrated that the two-dimensional elbow model and its coupling with the two-dimensional axisymmetric pipe model can be used to analyze the flow in a pipe loop consisting of straight pipes, elbows, and other components connected in series. The loop can be subject to two arbitrary pressure pulses at both ends. The pipe and component walls can be either rigid or elastic-plastic, but the elbow walls can only be rigid.

The sample problems have further demonstrated that inside the elbow the pressures may reach high levels because of the centrifugal forces and that the velocities inside a valve are nonuniform. These indicate that the one-dimensional methods are inadequate in predicting the fluid dynamics inside a loop component such as the elbow and valve.

It can also be concluded that plastic deformation of the walls attenuates the pressure pulse and changes its shape. The use of rigid and elastic wall assumptions in predicting the pressure wave propagation in a pipe, as in the conventional methods, leads to overestimated pressures.

Although the results of sample problem 1 indicated that the plastic deformation is limited to a short distance near the source pressure, it should be noted that the situation is completely different when a loop is subjected to two pressure pulses at both ends as has

TABLE I.

Dimensions of Loop Components*

Pipe, 3" OD x 40 mil		Elbow		
No.	Length, in.	No.	Total Angle, degree	Radius of Curvature, in.
1	7.5	1	90	4.5
2	12	2	90	4.5
3	18	3	90	4.5
4	54	4	180	4.5
5	24	5	90	4.5
6	12			

*1/10th-scaled model

been demonstrated in sample problem 4. The reason is that when the two pulses meet in the middle of the loop, a new pulse that may cause plastic deformation is formed there.

Like all the other numerical techniques, the results of the analysis are correct only within the framework of the assumptions, experimental verification is required to evaluate the effects of ignoring the secondary flow inside the elbow and the coupling of the elbow model with the pipe model. Experimental results that could be used for that purpose are not available, though some are planned in the near future [7].

However, a parametric study of the effects of different values of the ratio of the elbow radius of curvature to pipe diameter on the pressures inside the elbow has shown that the pressures, as well as the pressure differences in the radial direction inside the elbow, decrease with the increase of this ratio. This is to be expected, because the elbow approaches to a straight pipe with the increase of such ratio [8].

For the elastic-plastic straight pipes, Stanford Research Institute (SRI) had performed tests in which the pressure histories as well as the pipe wall deformation, were measured at different locations. The results obtained from the implicit ICE method showed good agreement with the experimental measurements.

References

[1] MONEIM, M. T. A.,"ICEPEL, a Two-dimensional Computer Program for the Transient Analysis of a Pipe-elbow Loop," Argonne National Laboratory report (to be published).

[2] HARLOW, F. H., and AMSDEN, A. A.,"A Numerical Fluid Dynamics Calculation Method for all Flow Speeds,"J. Computational Physics, 8 (1971), 197-213.

[3] CHANG, Y. W., and GVILDYS, J., "Analysis of the Primary Containment Response Using a Hydrodynamic-elastic-plastic Computed Code," Nucl. Eng. Des., 27, pp. 155-175, (1974).

[4] WANG, C. Y., "An Implicit Eulerian Method for Calculating Fluid Transients in Fast Reactor Containment," Argonne National Laboratory report (to be published).

[5] FLORENCE, A. L., and ABRAHAMSON, G. R., "Simulation of a Hypothetical Core Disruptive Accident in a Fast Flux Test Facility," HEDL-SRI-1, May 1973.

[6] CHEN, W. L., THOMPSON, D. H., and SHIN, Y. W., "NAHAMMER, A Computer Program for Analysis of One-dimensional Pressure-pulse Propagation in a Closed Fluid System," ANL-8059, May 1974.

[7] NAGUMO, G., personal communication, March 1975.

[8] Reactor Development Program Progress Report, ANL-RDP-38, March 1975.

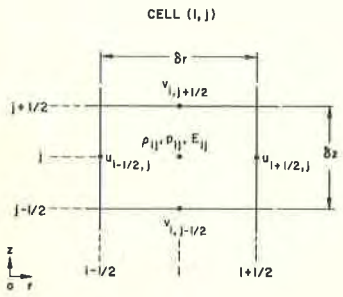

Figure 1 The Location of the Cell Variables in a Eulerian Computational Cell

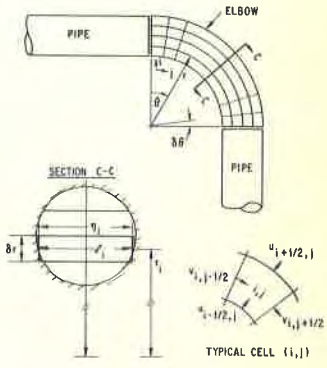

Figure 2 Mathematical Model of the Elbow and the Eulerian Mesh

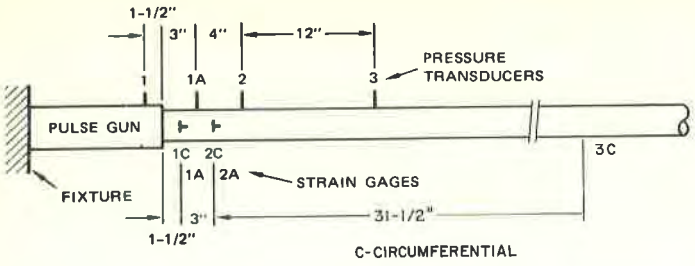

Figure 3 Configuration of the Elastic-Plastic Pipe

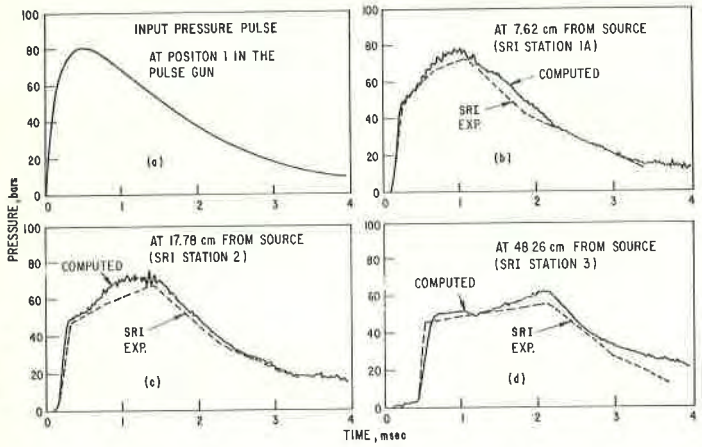

Figure 4 The Input Pressure Pulse and Computed Pressure Histories at Various Locations in the Elastic-Plastic Pipe

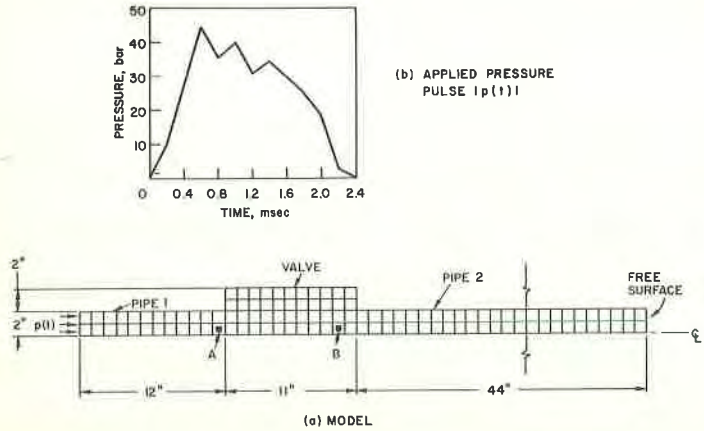

Figure 5 Mathematical Model of a Simple Valve System

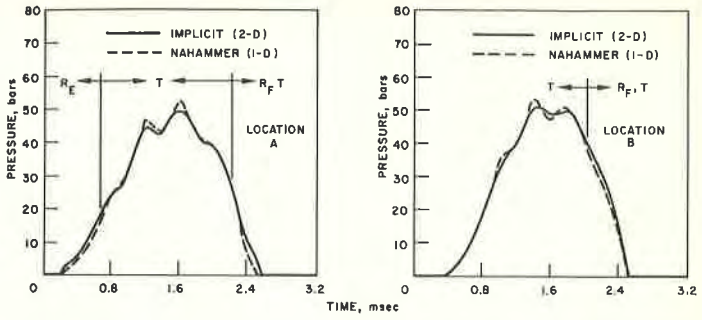

Figure 6 Pressure Pulses at Locations A and B in the Simple Valve System

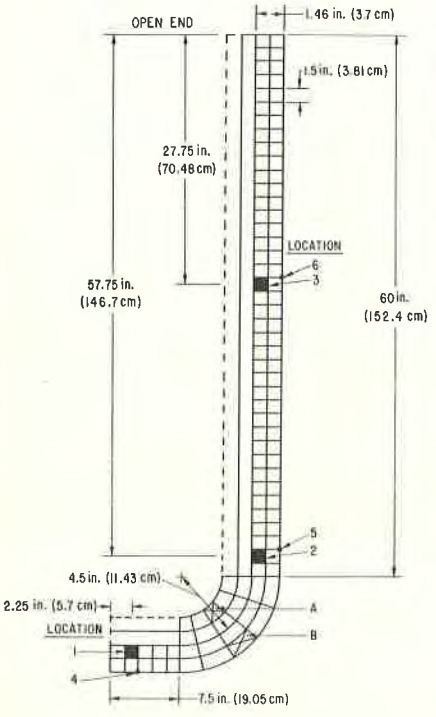

Fig. 7 a

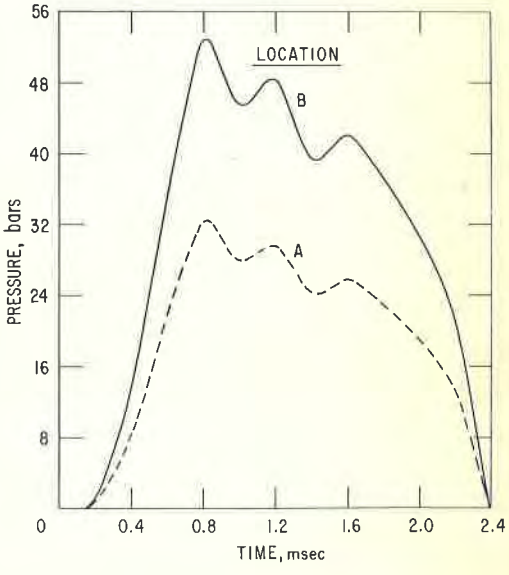

Fig. 7 b

Figure 7 Mathematical Model of the Elbow and Pressure Histories at Locations A and B Inside the Elbow

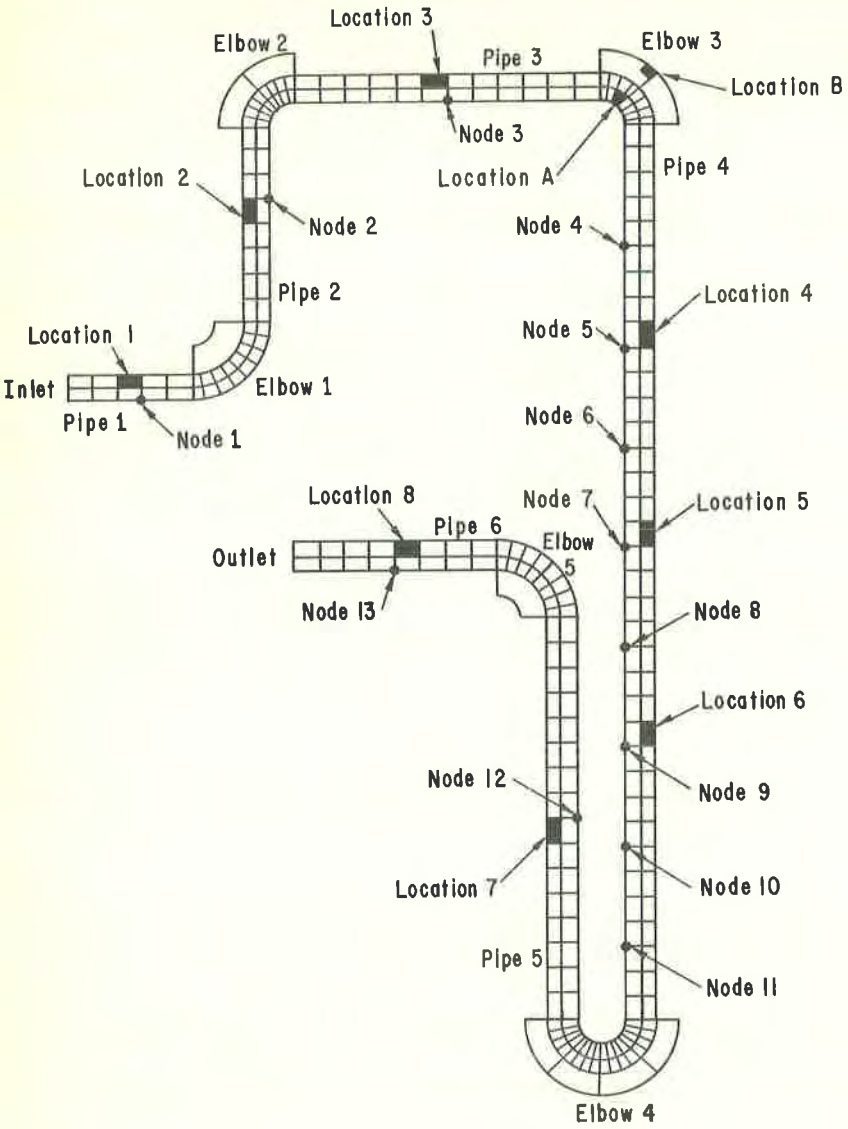

Figure 8 Mathematical Model of the Pipe-Elbow Loop

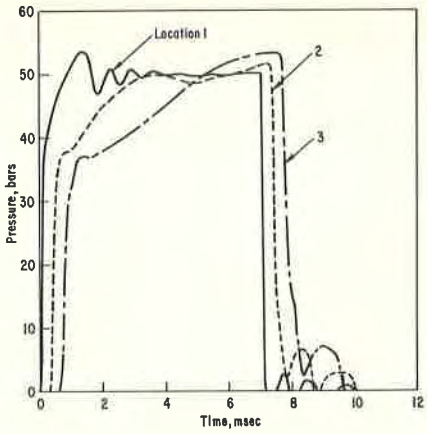

Fig.9 a

Figure 9 Pressure Histories at Various Locations in the Pipe-Elbow Loop

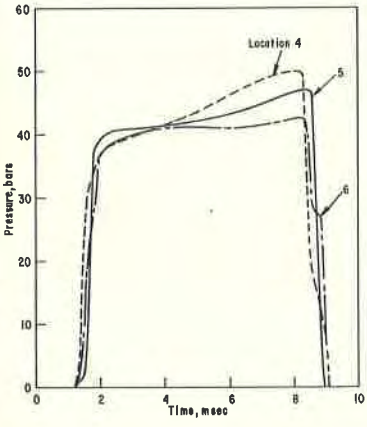

Fig.9 b

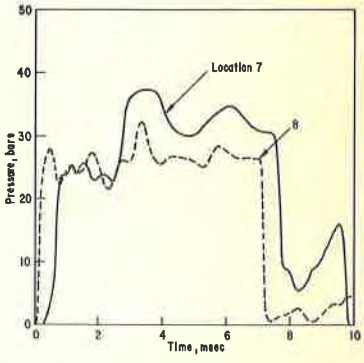

Fig. 9 c

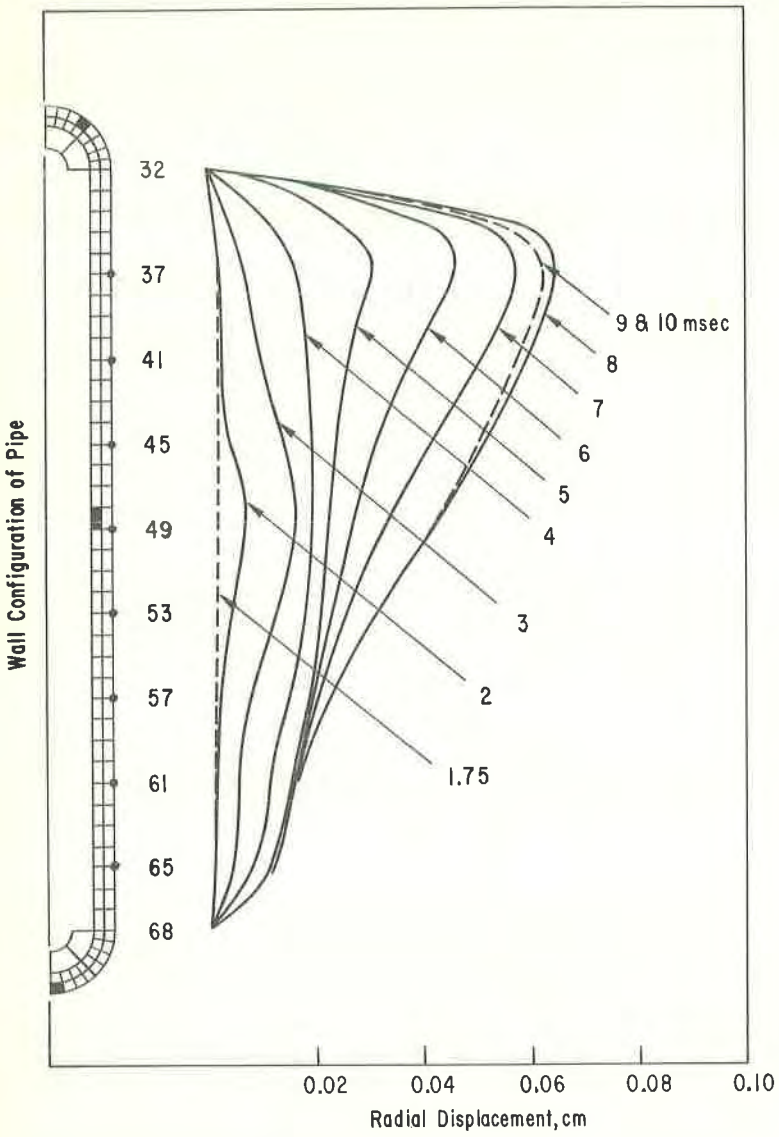

Figure 10 Wall Configuration of Pipe 4